Sensitivity analysis of cracking in large reinforced concrete structures: Case of the VeRCoRs mock-up

E-M. BOUHJITI[a,b,*], J. BAROTH[b], F. DUFOUR[b,c], B. MASSON[d]

a. Grenoble INP Partnership Foundation, Chair PERENITI, Grenoble, France
el-mahdi.bouhjiti@3sr-grenoble.fr / elmahdi.bouhjiti@gmail.com
b. Univ. Grenoble Alpes, CNRS, Grenoble INP[†], 3SR, F-38000 Grenoble, France
julien.baroth@univ-grenoble-alpes.fr
c. Head of the chair PERENITI (EDF SEPTEN/DTG/CIH), Grenoble, France
frederic.dufour@3sr-grenoble.fr
d. Electricité de France (EDF SEPTEN), Lyon, France
benoit.masson@edf.fr

Résumé :

L'objectif du présent article est d'étudier l'effet de la variabilité spatio-temporelle des propriétés mécaniques du béton sur sa fissuration. La stratégie proposée consiste à modéliser la fissuration par un modèle d'endommagement local régularisé en énergie de fissuration intrinsèque. Les effets d'échelle sont considérés, d'une part, par la réduction de la résistance à la traction en fonction du volume structurel d'intérêt et, d'autre part, par la modélisation de la variabilité spatiale du module de Young par un champ aléatoire lognormal autocorrélé. La stratégie de modélisation est appliquée à la première levée du mur de confinement de la maquette VeRCoRs (le gousset). Suite à un premier calcul de référence au jeune âge, une analyse de sensibilité est menée afin d'analyser les effets de la variation du facteur de réduction de la résistance à la traction et des propriétés du champ aléatoire sur l'évolution de l'état d'endommagement à l'échelle du volume structurel représentatif du gousset.

Abstract:

This paper aims at studying and defining the influence of the spatial distribution of concrete's mechanical properties on its cracking patterns. The modeling of concrete's cracking is based on a continuous energy-regularized and strain-based local damage model. Statistical and energetic size effects at the structural scale are taken into account (a) by reducing the mean tensile strength of the considered concrete volume according to a deterministic ''universal law'' and (b) by defining an autocorrelated lognormal random field associated with the concrete's Young's modulus. The first part of this article deals briefly with the various descriptive equations of the Thermo-Mechanical (TM) behavior of concrete at early age. More interest is shown towards the considered hypotheses related to size effect and energy regularization strategies. The second part of this paper is an application of the proposed modeling strategy to the first lift of the VeRCoRs containment wall mock up (the gusset) in attempt to predict concrete cracking. In a final part, a sensitivity analysis is performed with regards to the effects of numerical and physical parameters related to size effect on crack initiation, opening and spacing at the scale of the gusset's Representative Structural Volume (RSV).

[*] Corresponding author
[†] Institute of Engineering Univ. Grenoble Alpes

Key words: Reinforced concrete, cracking, size effects, random fields

1 Introduction

The modeling of concrete's cracking is still a major issue amongst civil engineering community. In the case of homogeneously distributed stress loads, the distribution of voids and defaults in the concrete volume is one of the driving factors of crack initiation and localization. The way such heterogeneousness affects concrete's mechanical behavior is, up to this day, a subject of controversy. From a modeling point of view, the mathematical description of cracks at the structural scale has to take into account the random aspect of crack initiation and also the observed size effects associated with large concrete structures [1]. In this article, we are interested in early age cracking of concrete where only the distribution of voids in the volume and the evolution of the mechanical property define the risk of cracking. Indeed, during early age phase and under endogenous conditions, the tensile stresses in concrete are self-induced and occur without any macroscopic stress concentration (in the absence of geometric singularities). This allows us to focus mainly on the accuracy of a numerical modeling of intrinsic defaults distribution using a continuous and macroscopic approach. After a brief description of the Thermo-Mechanical (TM) behavior of concrete at early age [2][3], we focus on the modeling of the various size effects and their associated descriptive equations. A blind calculation step is performed at the scale of the VeRCoRs gusset aiming at predicting its cracking state at early age. After assessing the differences between the model's and the observed results [4], a variance-based sensitivity analysis [5] is performed so as to identify the most influent parameters with regards to cracking and damage of concrete. The presented results cover only a portion of a more generalized and global analysis [6] that we have undertaken and intentionally focus on the random field parameters and their importance vis-à-vis the cracking pattern of concrete.

2 Modeling of concrete cracking

2.1 Thermo-mechanical coupling at early age

The thermal behavior of concrete is described according to the classical heat equation. A macroscopic approach is preferred to account for the exothermic nature of cement hydration [2][3]. Accordingly, an additional source term is added (Eq. 1) to describe the released heat during that phase [7]:

$$\rho_{hc} C_{hc}^{p} \frac{dT}{dt} - \lambda_{hc} \nabla^2 T = \frac{Q_\infty}{\zeta_\infty} \frac{d\zeta}{dt} e^{-\frac{E_a^{th}}{RT(t)}} \quad (1)$$

where ρ_{hc} (kg/m^3) is the hardened concrete's density, C_{hc}^{p} (J/kg/°K) and λ_{hc} (J/s/m/°K) are its thermal conductivity and thermal capacity respectively. The hydration parameters are the volumetric hydration heat Q_∞ (J/m3), the ultimate hydration rate ζ_∞, the hydration activation energy E_a^{th} (J/mol) and the universal gas constant R.

The dependence of the concrete's thermal properties on temperature and hydration rate is not considered in Eq. 1 as their effect on the computed temperature field remains negligible [8]. The drying of concrete is also neglected during the hydration phase and the hydration reaction is supposed to occur under endogenous conditions where concrete remains saturated.

The second step of calculations deals with the mechanical behavior of concrete. The temperature field is used as an input to define the endogenous and thermal shrinkages as well as the effect on the viscoelastic behavior of concrete. The concrete total strain is divided into four components:

$$\underline{\underline{\varepsilon_{TOT}}} = \underline{\underline{\varepsilon_{ELAS}}} + \underline{\underline{\varepsilon_{TH}}} + \underline{\underline{\varepsilon_{ES}}} + \underline{\underline{\varepsilon_{CR}}} \quad (2)$$

where $\underline{\underline{\varepsilon_{ELAS}}}$ is the elastic strain, $\underline{\underline{\varepsilon_{TH}}}$ is the thermal strain associated with temperature variation, $\underline{\underline{\varepsilon_{ES}}}$ is the endogenous shrinkage due to water reaction with cement [7] and $\underline{\underline{\varepsilon_{CR}}}$ is the creep strain.

In a saturated environment, concrete creep is only due to basic creep $\underline{\underline{\varepsilon_{BC}}}$. In this article, it is described according to the water migration theory [9]. Hence, the Burger model [10] is selected to define the viscoelastic behavior of concrete. It consists of series of Kelvin-Voigt (KV) and Maxwell (M) chains as shown in Fig. 1.

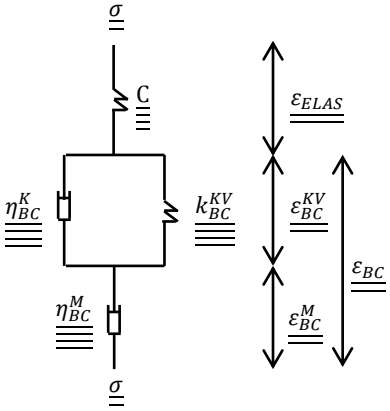

Fig. 1: Burger rheological model for concrete's basic creep

where $\underline{\underline{C}}$ is the compliance tensor depending on the Young's modulus E and the elastic Poisson ratio ν_{ELAS}. $\underline{\underline{\eta_{BC}^{KV}}}$ is the Kelvin chain viscosity tensor associated with basic creep, $\underline{\underline{k_{BC}^{KV}}}$ is the Kelvin chain rigidity tensor and $\underline{\underline{\eta_{BC}^{M}}}$ is the Maxwell chain viscosity tensor.

The increase of the elastic properties of concrete as well as the decrease of its viscoelastic properties due to its hardening are modeled using the maturity method [11][12]. The effect of temperature on basic creep kinetic is modeled using the Arrhenius law which describes the thermo-activation of water diffusion in capillary voids [13].

2.1.2 Damage description and coupling with creep

Compared to non-local damage modeling approaches [14][15], local damage models are considerably less time consuming and seem to be more accurate for the modeling of large structures with a reasonably refined finite elements mesh. In this article, the isotropic unilateral μ-Mazars damage model [16] is used (Eq. 3) where the damage variable d depends on a given equivalent strain (Eq. 4). In order to take into account the contribution of basic creep to the observed damage, a portion of basic creep strain is considered whilst computing the equivalent strain [17] (Eq. 4).

$$\underline{\underline{C}} = (1 - d)\underline{\underline{C_0}} \quad (3)$$

$$\varepsilon_{eq,t} = \left|\left|\underline{\underline{\varepsilon_{ELAS}}} + \beta_{coupl}\,\underline{\underline{\varepsilon_{CR}}}\right|\right|_t \qquad \varepsilon_{eq,c} = \left|\left|\underline{\underline{\varepsilon_{ELAS}}} + \beta_{coupl}\,\underline{\underline{\varepsilon_{CR}}}\right|\right|_c \quad (4)$$

where $\underline{\underline{C_0}}$ is the initial compliance tensor (undamaged) and d the isotropic damage variable. $||.||_t$ and $||.||_c$ are a given mathematical norms under tensile and compressive loads respectively. β_{coupl} is the

coupling factor between damage and creep (between 0 and 1 – 0 means that creep does not contribute at all to concrete damage and 1 means that all creep strain is considered while computing damage).

Finally, an additional post-processing step is required to define equivalent crack openings from the observed equivalent strains. The terms equivalent crack strain ε^{uco} and equivalent crack opening u_{ck} are preferred to emphasize the equivalence between a real crack in a discontinuous domain and its equivalent crack in a continuous one. The used formula (Eq. 5) is a generalization of the initial 1D crack strain in [18].

$$u_{ck} = h_{EF} * \varepsilon^{uco}$$
$$\varepsilon^{uco} = \left|\left| \underline{\underline{\varepsilon_{\mathrm{ELAS}}}} + \beta_{\mathrm{coupl}}\, \underline{\underline{\varepsilon_{BC}}} - \frac{(1+\nu_{ELAS})\underline{\underline{\sigma}} - \nu_{ELAS}\, tr\left(\underline{\underline{\sigma}}\right)\underline{\underline{I}}}{E} \right|\right| \quad (5)$$

where h_{EF} is the characteristic length of the finite element $h_{EF} = \sqrt[3]{V_{EF}}$ and $\left|\left|\boldsymbol{X}\right|\right| = \max(X_I, X_{II}, X_{III}, 0)$ with X_I, X_{II}, X_{III} are the Eigen values of a given tensor $\boldsymbol{X}$.

2.2 Modeling of size effect

Local damage models are mesh-dependent as the dissipated energy per finite element depends on its size. To avoid such dependency, the computed post-peak behavior should vary with the finite element size. Hereafter, the Hillerborg energy based regularization technique [19] is applied to the used damage model. Moreover, the tensile strength of concrete is defined according to a ''universal'' size effect law where the effective volume under tensile stresses is considered. Lastly, the statistical size effect is described by using random fields to model the spatial distribution of the concrete's Young's modulus.

2.2.1 Energy based regularization technique

According to the Hillerborg energy based regularization principle, both the dissipated fracture energy and tensile strength should not depend on the characteristic length of the finite element h_{EF} (Eq. 6):

$$\frac{\mathrm{G_F}}{\mathrm{E}\, h_{EF}} = \frac{\mathrm{f_t^2}}{2\,\mathrm{E}} + \int_{\frac{\mathrm{f_t}}{\mathrm{E}}}^{\infty} (1-\mathrm{d})\varepsilon\, \mathrm{d}\varepsilon \quad (6)$$
$$\sigma \leq f_t \quad \forall \varepsilon$$

where $\mathrm{G_F}$ (N.m) is the fracture energy of concrete and $\mathrm{f_t}$ (Pa) is its tensile strength.

The analytical solution of the previous system of equations (Eq. 6) exists and can be derived manually. However, it remains relatively complicated and not practical for engineering use. For that reason, the regularization is applied to the intrinsic fracture energy only $\mathrm{G_f}$. It refers to the energy that is actually dissipated ahead of the crack tip and controls the propagation of the crack. It corresponds to about 40 % of the total fracture energy $\mathrm{G_F}$ [20]. This reduces the number of equations to solve since by definition the yield strength becomes equal to the ultimate tensile strength of concrete and the area under the behavior law is accordingly smaller as depicted in Fig. 2.

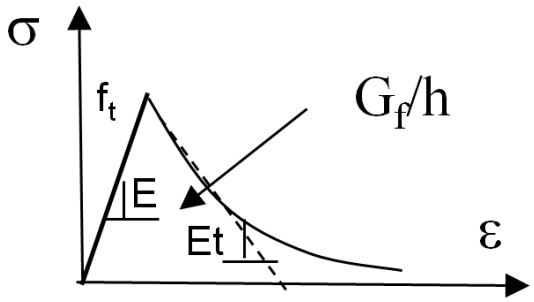

$$0 \le h \le 0.8\frac{G_F}{E}\left(\frac{E}{f_t}\right)^2 \qquad B_t = \frac{E}{f_t} + \frac{\frac{E}{f_t}\,h}{0.8\frac{G_F}{E}\left(\frac{E}{f_t}\right)^2 - h} \tag{7}$$

Fig. 2: Intrinsic energy based regularization technique applied to the µ-Mazars [16] where B_t is a parameter that defines the shape of the post-peak behavior law under tensile loads

2.2.2 Size effect '' universal law ''

According to Weibull theory, the tensile strength of concrete is related to the considered volume as following [1]:

$$\frac{f_t(V_{eff})}{f_{t,ref}} = \left(\frac{D_{eff}}{D_{ref}}\right)^{-\frac{n}{m}} \tag{8}$$

where m is the Weibull modulus, $f_{t,ref}$ is the tensile strength measured on a given reference dimension D_{ref}, D_{eff} is the effective structural dimension under tensile loads and n is a dimensional factor (n=1 for 1D,2 for 2D or 3 for 3D).

Hereafter, the 3D configuration is considered. Similar developments can be derived for the 1D and 2D cases. In general terms, the effective volume V_{eff} writes:

$$V_{eff}(\overrightarrow{x_0}) = \int_\Omega \psi\left(|\vec{x} - \overrightarrow{x_0}|, l_c, \left|\left|\underline{\underline{\sigma_+}}(\vec{x})\right|\right|\right) d\Omega \tag{9}$$

where ψ is a weight function defining the zone of influence on a given point $\overrightarrow{x_0}$ depending on an internal length l_c and the surrounding tensile stresses $\underline{\underline{\sigma_+}}$. However, it is possible to simplify the previous equation under homogeneous loads into Eq. 10 which is only descriptive of the distribution of defaults and voids in the volume and its effect on the tensile strength reduction:

$$V_{eff}(\overrightarrow{x_0}) = \int_\Omega \psi(|\vec{x} - \overrightarrow{x_0}|)\, d\Omega \tag{10}$$

with $\psi(|\vec{x} - \overrightarrow{x_0}|) = e^{-\frac{1}{2}\left(\frac{|\vec{x}-\overrightarrow{x_0}|}{l_c}\right)^2}$ chosen subjectively as a Gaussian quadratic weighing function [21]. To ensure objectiveness with regards to the choice of the weighing function, the internal length l_c has to be changed in order to verify Eq. 11.

$$\int_{-\infty}^{+\infty} \psi(x, l_c)\, dx = D_{eff,\infty} = c^{ste} \quad \forall\psi \tag{11}$$

where $D_{eff,\infty}$ is what we can call the scale length (objective value) to be identified experimentally. For the Gaussian quadratic function, l_c writes $D_{eff,\infty} = \sqrt{2\pi}\, l_c$.

2.2.3 Statistical size effect

The heterogeneousness of concrete can be described by the spatial variability of its Young's modulus [22] or of its tensile strength [21] at the scale of the Representative Volume Element (Equivalent

Homogenized Material). However, the two mechanical properties do not follow the same probability density function. The first parameter follows rather a lognormal distribution whereas the second follows a Weibull type density function. From a mathematical point of view, the spatial correlation of gaussian and lognormal fields is easier and does not require any further transformations. For that reason, the statistical size effect is modeled in our study by a random field associated with the Young's modulus whereas the reduced tensile strength is considered constant. The autocorrelation (spatial correlation) of the random field is performed following the Karhunen-Loève decomposition [23] and the covariance between two points $\overrightarrow{x_i}$ and $\overrightarrow{x_j}$ writes:

$$C(\overrightarrow{x_i}, \overrightarrow{x_j}) = \sigma^2 \, e^{-\left(\frac{|\overrightarrow{x_i} - \overrightarrow{x_j}|}{l_{ac}}\right)^2} \tag{12}$$

where σ^2 is the associated variance of the random field and l_{ac} the autocorrelation length associated with the Gaussian quadratic autocorrelation function (here considered the same in all principal directions). In the case where another autocorrelation function ρ [24] is selected‡, the autocorrelation length l_{ac} has to be changed so as to verify Eq. 13 where the fluctuation length l_{flu} (objective value) is considered:

$$\int_{-\infty}^{+\infty} \rho(x, l_{ac}) \, dx = l_{flu} = c^{ste} \quad \forall \rho \tag{13}$$

3 Application: Damage analysis of VeRCoRs gusset

3.1 Overview

VeRCoRs is a 1:3 scale mock-up of a double walled Nuclear Containment Building (NCB) [4]. The inner wall is made out of reinforced and prestressed concrete (Fig. 3a) and ensures most of the static containment. In this article, we are focusing on the behavior of the first lift of the containment wall (the gusset – Fig. 3b). During the early age phase, tensile stresses develop in the gusset volume because of (a) the cooling of concrete after hydration ends, (b) the strain gradient in the concrete thickness due to endogenous and thermal shrinkages and (c) the restrained strains due to the presence of a lower massive already erect base slab. Eventually, the risk of cracking in this area of the NCB is higher and requires an in-depth analysis of the parameters responsible for concrete damage.

(a) (b)

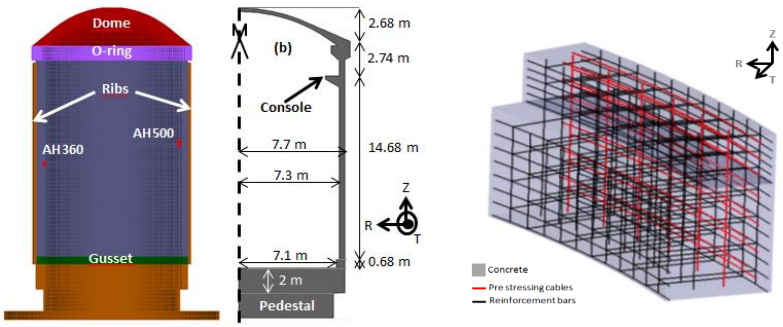

	Concrete	Steel
FE	3D Quadratic	1D Linear
h_{EF}	4 - 7 cm	

Fig. 3: (a) General 3D and 2D-AXIS views of the VeRCoRS mock-up (b) 3D view of the gusset (15° revolution angle)

3.2 Numerical analysis

‡ Compared to other autocorrelation functions such as the linear and sinusoidal types and based on a sensitivity analysis we performed using 30 realizations of independent and different random fields, the Gaussian quadratic function seems to minimize the most boundary effects on the cracking patterns (less occurrences of cracks nearby the boundaries – Fig. 5).

3.2.1 Numerical experimental design

Only the variables of interest are detailed in this article (Tab. 1). Further numerical inputs and experimental results are available in [8][4][6]. The mean tensile strength of VeRCoRs hardened concrete is about 4.3 MPa (splitting test [NF EN 206-1]), its mean Young's modulus value is around 36 GPa and the fracture energy is around 77 N.m. The observed distribution of the Young's modulus values is of a lognormal type (Fig. 4a) with a coefficient of variation around 10 % (the associated Weibull modulus m is 12). At the structural scale, however, the tensile strength of concrete is expected to be less than the one measured at the specimen scale (Eq. 14). In the case of a splitting test, the effective volume seems to be around 300 cm^3 regardless of the scale length in Eq. 15 [21]. The reference dimension is hence $D_{ref} = 6.70$ cm. In the absence of sufficient data at the specimen scale of VeRCoRs concrete, the internal length l_c is *a priori* considered equal to 50 cm [21] (around 30 times the maximal aggregate size). In other words, the scale length $D_{eff,\infty}$ is equal to 17 cm (around 10 times the maximal aggregate size). Accordingly, the tensile strength of VeRCoRs gusset should be reduced by about $\beta_{red} = 1 - \frac{f_{t,eff}}{f_{t,ref}} = 35$ % (Fig. 4b). Finally, the autocorrelation length l_{ac} is considered *a priori* equal to the internal length l_c. This is actually in line with the usual fluctuation lengths l_{flu} associated with the Young's modulus (around 1 m [22]).

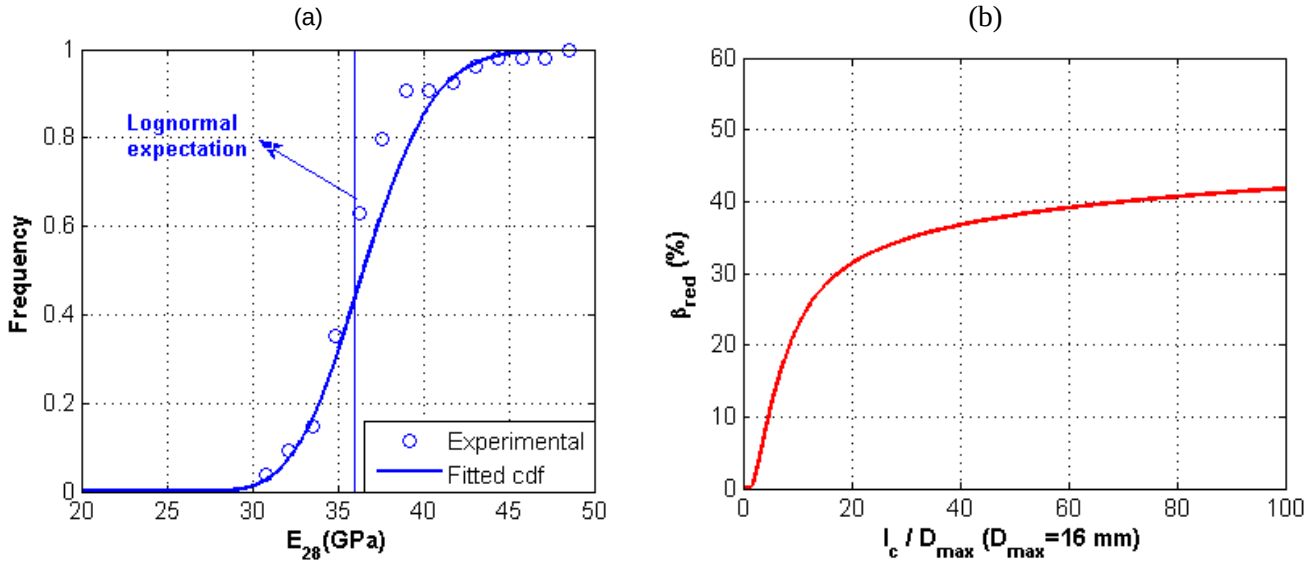

Fig. 4: (a) Lognormal CDF of the Young's modulus values (b) Size effect '' universal law '' applied to the VeRCoRs gusset

Parameter	Symbol	Unit	Reference	CV (%)	
Young modulus	E	GPa	36	10	Observed
Tensile strength	$f_{t,ref}$	MPa	4.3	10	
Fracture energy	G_F	N/m	77	10	
Objective internal length	$D_{eff,\infty}$	m	0.17	50	Expert judgment
Coefficient of variation associated with the random field	$CV_E = \frac{\sigma_E}{\mu_E}$	%	10	50	
Fluctuation length	l_{flu}	m	1	50	

Tab. 1 : Mechanical properties and size effect parameters for VeRCoRs concrete

Besides the list of parameters presented in this article, there are 21 additional mechanical properties that are considered in this analysis [6] but will not be detailed hereafter for the sake of consistency.

3.2.2 Variance based sensitivity analysis

The variance based sensitivity analysis is a global sensitivity analysis that aims at decomposing the model's variance into partial contributions of each input as well as the interactions between all inputs. Given the high number of inputs (27 parameters) and the required computational time for every simulation (12 hours), it seems more reasonable to identify the most important parameters, overlooking the eventual interactions and correlations, before computing higher order sensitivity analyses such as the classical collocation and perturbation methods or aiming at a probabilistic coupling [24]. The OFAT (One-Factor-At-a-Time) method is a first step to achieve that goal with the least computational cost.

Hence, for a given input X_i, the first order sensitivity index writes [5]:

$$0\ \% \ \leq \ \delta_i = \frac{\mathrm{Var}[Y_{i-}, Y_0, Y_{i+}]}{\sum_j \mathrm{Var}[Y_{j-}, Y_0, Y_{j+}]} \leq \ 100\ \% \tag{20}$$

where Y_0 is the model's response using the mean values of inputs, Y_{i-} (and Y_{i+}) is the model's response with a decreased (increased) value of the input X_i by a given coefficient of variation CV_i.

$$X_{i+} = (1 + CV_i)X_i \qquad X_{i-} = (1 - CV_i)X_i \tag{21}$$

However, since the input parameters are not associated with the same coefficients of variation, Eq. 20 needs to be normalized for better objectiveness. The index δ_i which is used in this study is shown in Eq. 22. We are also considering two other indices δ_{i+} and δ_{i-} for quantitative analysis of the TM parameters effect which are simply the relative differences between the reference response Y_0 and Y_{i-} or Y_{i+} (Eq. 23).

$$0\ \% \ \leq \ \delta_i = \frac{\frac{\sqrt{\mathrm{Var}[Y_{i-}, Y_0, Y_{i+}]}}{CV_i}}{\sum_j \frac{\sqrt{\mathrm{Var}[Y_{j-}, Y_0, Y_{j+}]}}{CV_j}} \leq \ 100\ \% \tag{22}$$

$$\delta_{i-} = -\frac{\frac{Y_{i-} - Y_0}{Y_0}}{CV_i} \qquad \delta_{i+} = \frac{\frac{Y_{i+} - Y_0}{Y_0}}{CV_i} \tag{23}$$

The variables of interest Y in this paper are the following:

Variable of interest	Symbol
Instant of crack initiation	Y_1
Mean crack opening	Y_2
Number of cracks	Y_3
Mean spacing between cracks	Y_4

Tab. 2 : Variables of interest

3.2.3 Numerical results

The mechanical calculation step applied to the VeRCoRs RSV lasts about 12 hours and covers the whole phase preceding the operational phase of the VeRCoRs NCB. The obtained results are presented hereafter:

- **Deterministic analysis:** In Fig. 5 the obtained numerical cracking patterns are described according to parameters in Tab. 1. Based on 30 various and independent random fields, three cracking

patterns seem to be recurrent: the number of cracks varies between 1 and 2 per RSV and the spacing value between 15° and 5°. For each cracking pattern the crack opening values vary scarcely. The crack initiation time is around 3-4 days and does not seem to depend on the generated random field. As for numerical crack opening values, they are about 37-60 µm and seem to propagate from the inner side towards the outer one. Based on visual inspection results at 4 days after casting [4], VeRCoRs gusset inner cracks have a mean spacing of 10° (there are 18 cracks at 5 days) with openings inferior to 100 µm (measuring device precision). At 12 days after casting, the number of cracks increases on the intrados by 4 whereas on the extrados of the gusset the number of cracks is of 24 (15° average spacing). The numerical results are therefore in line with the in situ observations (Fig. 6). However, computing 30 random fields is not enough to have a concluding idea with regards to the effect of the random field on crack spacing values and their associated probability density function. Given the required computational time, it seems impractical to use Monte Carlo methods. We are currently working on finding out a better suited analysis strategy. In the framework of this article, however, this aspect is overlooked in order to focus on the parameter defining the random field for a given generation. For that reason, the uncorrelated random field is the same for all the succeeding simulations and corresponds to the one of the first cracking pattern in Fig. 5 (two centered cracks).

Young's modulus random field E (GPa)	Cracking pattern (1 week after casting - u_{ck} (m))	Crack opening profile through the gusset's thickness u_{ck} (m)
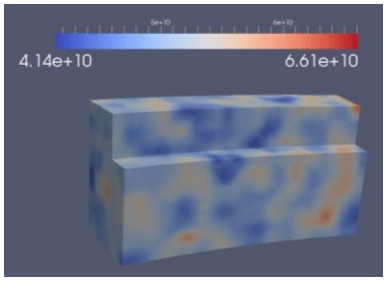	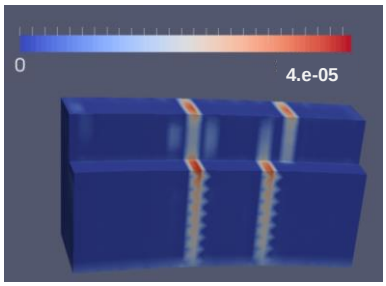 Number of occurrences: 7/30	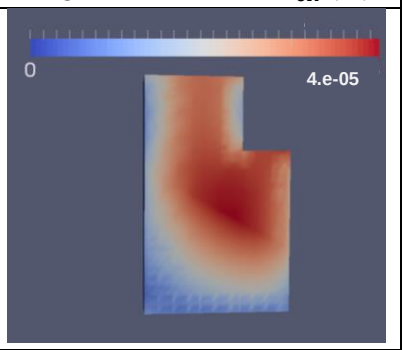
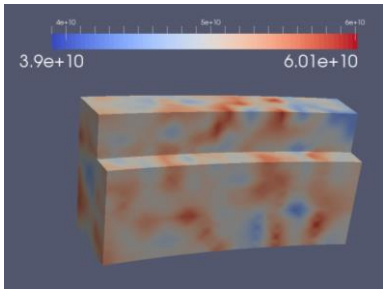	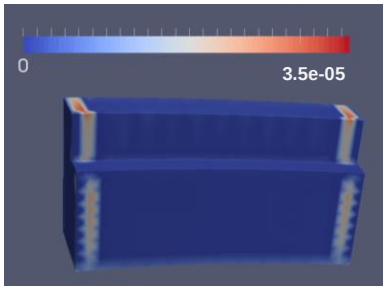 Number of occurrences: 6/30	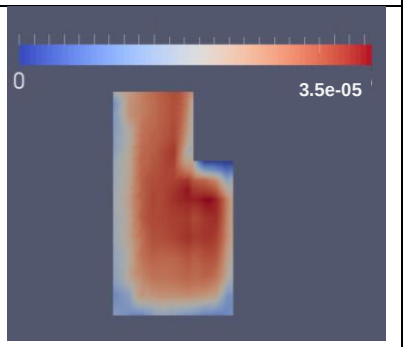
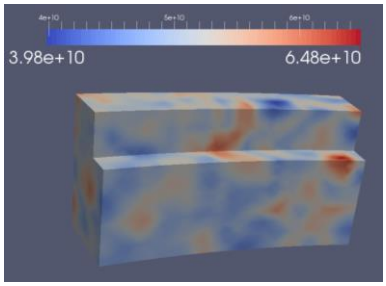	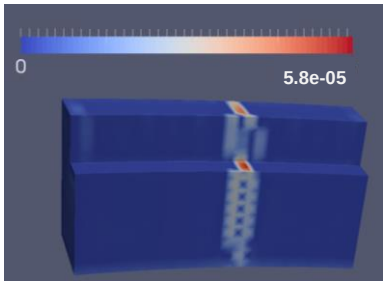 Number of occurrences: 17/30	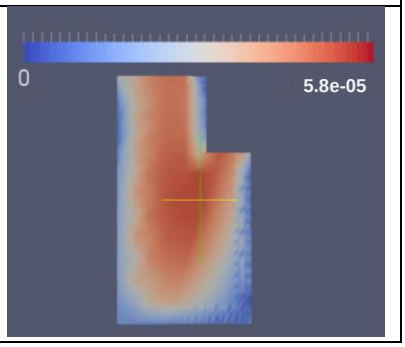

Fig. 5: Numerical cracking patterns of VeRCoRs gusset 1 week after casting

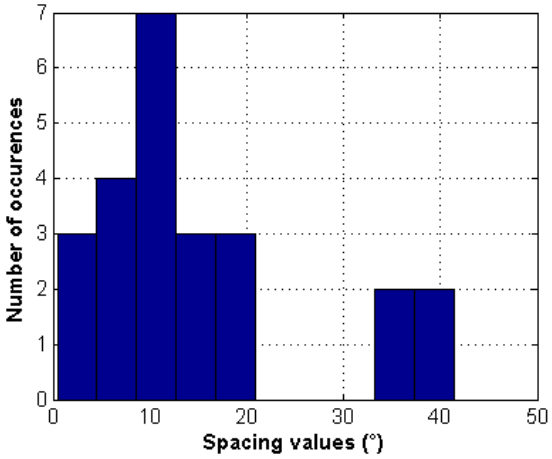

Fig. 6: In situ observations of crack spacing values on the extrados 12 days after casting

- **Sensitivity analysis:** In total, there are 55 simulations (2 for each input parameter in addition to the reference simulation). In Tab. 1 two inputs ($D_{eff,\infty}$ and l_{flu}) are issued from the literature whereas the others (E, f_t, G_F and CV_E) have an intrinsic variations associated with the concrete's heterogeneousness. This obviously has an effect on the model's response and might change the crack initiation and spacing. Hence, two questions arise: (a) what are the most influent size effect parameters with regards to cracking? And (b) Are the obtained numerical results accurate enough compared to the experimental ones considering the intrinsic variation of the concrete's properties and the scattering of in situ observations?

Fig. 8 and Fig. 9 sum up the obtained results and show the obtained variations of the considered 1st order sensitivity indices for the parameters in Tab. 1. In Fig. 8a the evolution of the mean crack opening value in time is plotted for the considered min and max values of each parameter. Based on Fig. 8b, it seems that parameters in Tab. 1 represent about 80 % of the total variance when it comes to crack initiation with more than 45 % associated with the size effect reduction ratio. This result is expected as the concrete's yield strain f_t/E is directly affected. On the other hand, crack spacing seems to be more dependent on the mean Young's modulus and the tensile strength values rather than on the other parameters defining the random field ($D_{eff,\infty}, l_{flu}, G_F$ and CV_E). As for the average crack opening values, random field properties seem to affect it less compared to the classical mechanical properties of concrete (Young modulus, tensile strength, shrinkage coefficients and creep parameters).

Coming back to our reference simulation (Fig. 5 – cracking pattern with two centered cracks), it seems that the increase of the Young's modulus or the decrease of the tensile strength by 10 % lead to a 60 % increase in the crack opening values (Fig. 9). By analyzing the post-peak behavior for such variations (Fig. 7), concrete behavior becomes more brittle which justifies the increase in crack opening values at crack initiation and also the reduction of cracks number.

According to Fig. 9, even by increasing the scale length $D_{eff,\infty}$ (in Eq. 11) by 50 % (due to size effect), in other words by increasing the reduction factor β_{red}, the crack initiation time seems to be the same. On the contrary, when the effective tensile strength is increased (50 % decrease of $D_{eff,\infty}$), the general behavior of the gusset is enhanced leading to delayed cracking. This is probably due to the way stirrups and reinforcement bars are modeled in our analysis (1D elements within the volume) which eventually induces a general increase of the equivalent Young's modulus at the Gaussian points level (compared to the Young's modulus of concrete) and limits the effect of the tensile strength reduction on the yield strain. However, the increase of concrete's yield strain can only increase the equivalent Young's modulus values at the Gauss point level which leads to delayed crack initiation.

The fluctuation length seems to have more effect on the maximum crack opening than on the number of cracks at the RSV scale. By choosing a smaller fluctuation length, the scattering of the random field is higher. Therefore the chances of having smaller cracking threshold are bigger and so are the chances to exceed the yield strain or the damage threshold (Eq. 5).

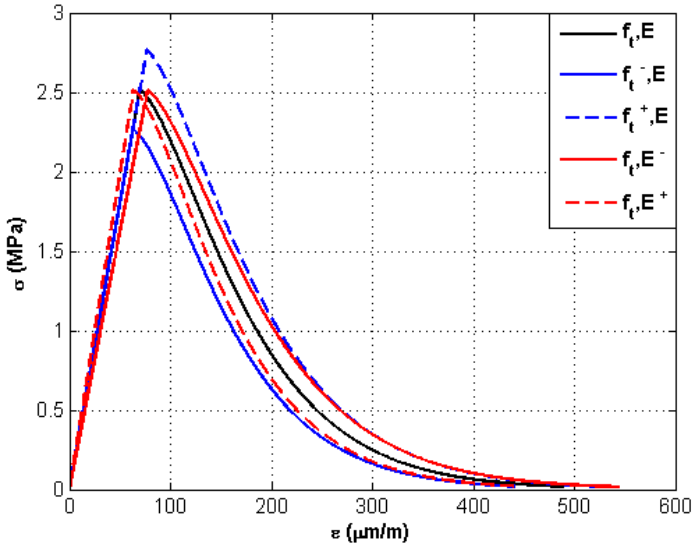

Fig. 7: Effect of the variation of Young's modulus and tensile strength values on the implemented behavior law (Gauss point level)

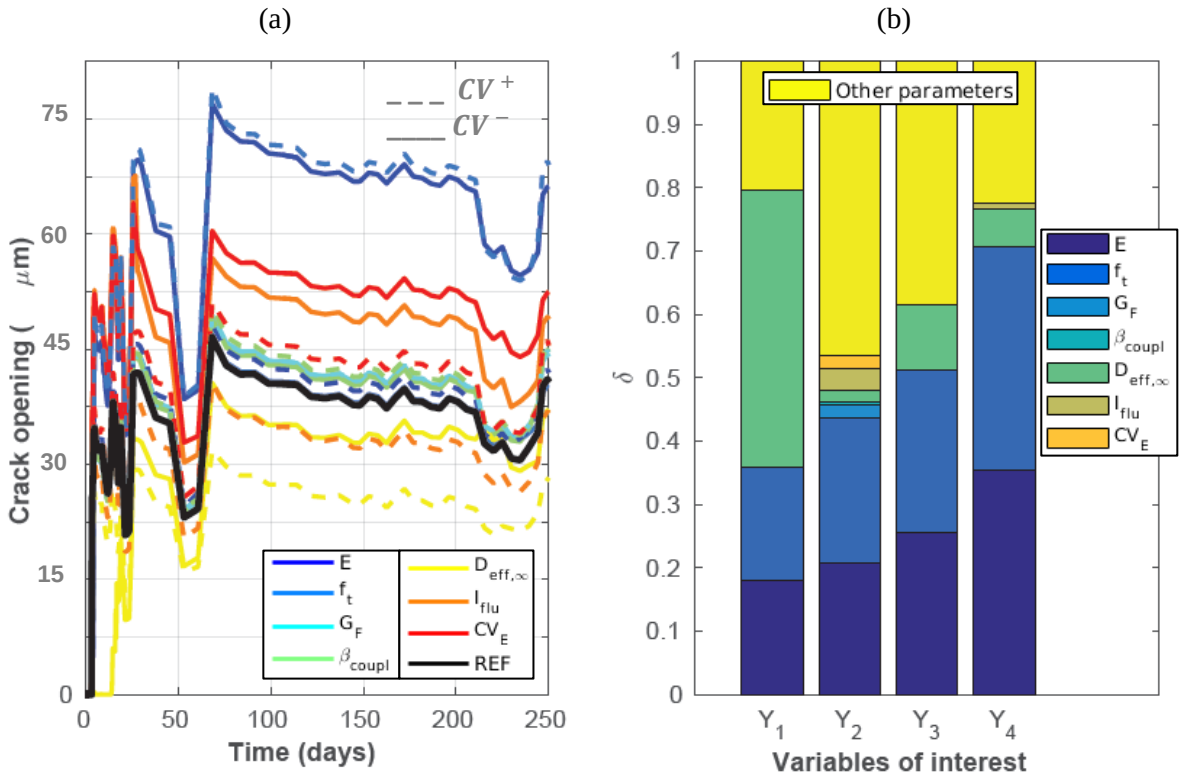

Fig. 8: (a) Average crack opening evolution with time for all parameters in Tab. 1 (b) Contribution of the input parameters to the total variance of the variables of interest in Tab. 2

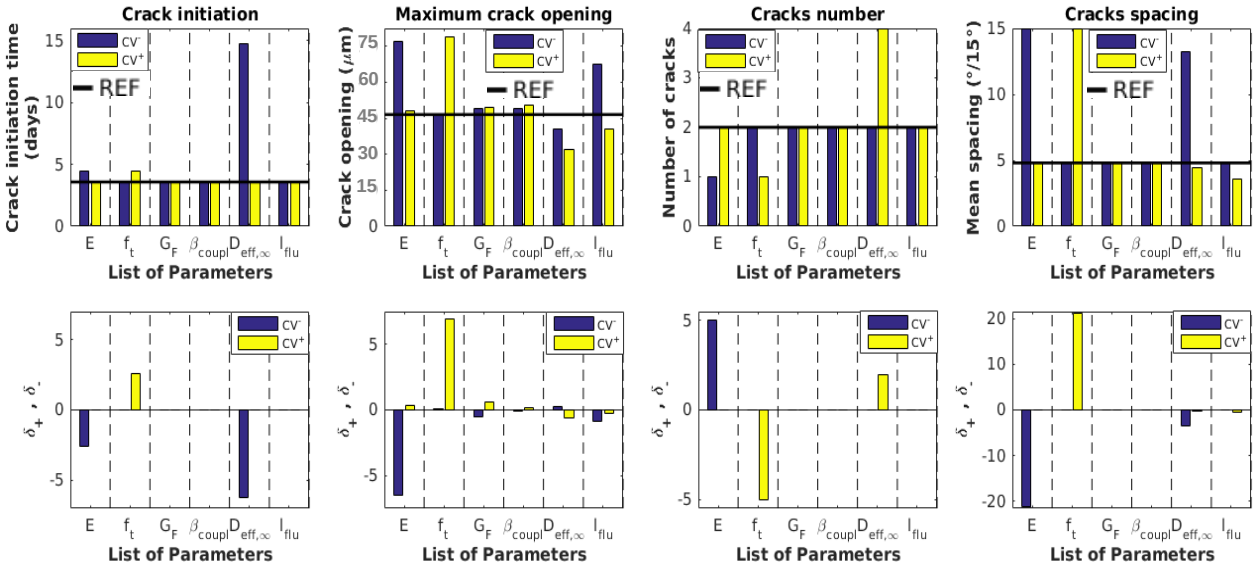

Fig. 9: Numerical relative differences due to the inputs variation

3 Conclusions

In conclusion, and to answer our two main questions:

- For a given lognormal random field, it seems that the mean values of Young's modulus and the tensile strength of concrete are key parameters with regards to crack opening values and crack spacing (Fig. 8 – Fig. 9). These parameters define the damage threshold but also define the brittleness of concrete (Eq. 7 – Fig. 7). Accordingly, for a given constant fracture energy, the reduction of the Young's modulus or the increase of the tensile strength leads to less cracks and higher crack opening values. The same number of cracks and the same crack opening values are obtained when the yield strain (which is equal to the tensile damage threshold) is increased (E increased or f_t decreased). The reduction factor of the tensile strength associated with size effect β_{red} seems to have more effect on the number of cracks as its value increases and on crack initiation time as it decreases. For the considered variation domains, concrete's fracture energy, the fluctuation length and the variance associated with the random field scarcely affect the cracking pattern of concrete.
- Eventually, we have demonstrated by numerical means that the cracking pattern of the gusset's RSV depends on the random field generation and that, from a predictive point of view, one deterministic analysis does not suffice to have a conclusive idea about the number of cracks or their spacing. However, for a given random field, the intrinsic variation of the Young's modulus (10 % increase) or the tensile strength (10 % decrease) and the increase of the scale length $D_{eff,\infty}$ (or its associated β_{red}) have direct effect on the cracking pattern. Our future work will be oriented towards the probabilistic description of our inputs in order to analyze the possible correlations between the most influent parameters and their combined effects on concrete cracking at early age.

Acknowledgements

This work was supported by EDF-SEPTEN/DTG/CIH within the Chair PERENITI agreement with the Grenoble INP Partnership Foundation. The author is grateful to EDF-SEPTEN for the provided in situ measurements. The Chair PERENITI partners shall not in any circumstances be deemed liable for the content of this publication which is only binding its author. The 3SR lab is part of the LabEx Tec 21 (Investissements d'Avenir - Grant agreement n°ANR-11-LABX-0030).

References

[1] Bažant Z.P. Size effect on structural strength: a review. Archive of applied mechanics 69 (1999) 703-725
[2] Conceição J., Faria R., Azenha M., Mamede F., Souza F. Early-age behaviour of the concrete
[2] Conceição J., Faria R., Azenha M., Mamede F., Souza F. Early-age behaviour of the concrete surrounding a turbine spiral case: Monitoring and thermo-mechanical modeling. Engineering Structures 81 (2014) 327-340
[3] Briffaut M., Benboudjema F., Torrenti J.M., Nahas G. Effects of early age thermal behaviour on damage risks in massive concrete structures. European Journal of Civil and Environmental Engineering 16(5) (2012) 589-605
[4] Corbin M., Garcia M. Benchmark VeRCoRS report 2015 (conference-service.com/edf-vercors/welcome.cgi)
[5] Sobol' I. M. Global sensitivity indices for nonlinear mathematical models and their Monte Carlo estimates. Mathematical and Computers in Simulation 55 (2001) 271 – 280.
[6] Bouhjiti E-M., Baroth J., Dufour F., Masson B. Sensitivity analysis of the Thermo-Hydro-Mechanical parameters affecting double walled Nuclear Power Plants behaviour at the representative structural volume scale. Transactions SMIRT-24, Korea, 2017.
[7] Ulm F.-J., Coussy O. Couplings in early-age concrete: From material modeling to structural design. International Journal of Solids and Structures 35(31) (1998) 4295-4311
[8] Bouhjiti E-M., Baroth J., Dufour F., Masson B. Damage analysis and prediction of air leakage rate in nuclear reactor containment structures: numerical model validation based on the VeRCoRS mock-up. Proceedings TINCE-03, France, 2016.
[9] Lohtia R.P. Mechanism of creep in concrete. Roorkee University Research Journal 12(1-2) (1970) 37–47
[10] Foucault, A., Michel-Ponnelle, S., Galenne, E. A new creep model for NPP containment behaviour prediction. International conference on Numerical modeling Strategies for sustainable concrete structures, 2012
[11] De Schutter G., Taerwe L. Degree of hydration-based description of mechanical properties of early age concrete. Materials and structures 29(6) (1996) 335-344
[12] De Schutter G. Degree of hydration based kelvin model for the basic creep of early age concrete. Materials and Structures 30(4) (1999) 260-265
[13] Bažant Z.P. Thermodynamics of interacting continua with surfaces and creep analysis of concrete structures. Nuclear Engineering and Design 20(2) (1972) 477-505
[14] Giry C., Dufour F., Mazars J. Stress based nonlocal damage model. International Journal of Solids and Structures 48(25-26) (2011) 3431-3443
[15] Peerlings R.H.J., de Brost R., Brekelmans W.A.M., Geers M.G.D. Gradient-enhanced damage modeling of concrete fracture. Mechanics of Cohesive-frictional Materials 3(4) (1998) 323-342
[16] Mazars, J., Hamon, F., Grange, S. A new 3D damage model for concrete under monotonic, cyclic and dynamic loadings. Materials and structures 48(11) (2015) 3779-3793
[17] Torrenti J.M., Nguyen V. H., Colina H., Le Maou F., Benboudjema F., Deleruyelle F. Coupling between leaching and creep of concrete. Cement and concrete research 38(6) (2008) 816 – 821
[18] Mattalah, M., La Borderie, C., Maurel, O. A practical method to estimate crack openings in concrete structures. International journal for numerical and analytical methods in geomechanics 34(15) (2010) 1615–1633
[19] Hillerborg A. Application of fracture mechanics to concrete – Summary of a series of lectures. 1988 Lund Institute of Technology.
[20] Planas J., Elices M., Guinea G.V. Measurement of the fracture energy using three-point tests. Part 2: influence of bulk energy dissipation. Materials and structures 25 (1992) 305 – 316
[21] Sellier A., Millard A. Weakest link and localisation WL2: a method to conciliate probabilistic and energetic scale effects in numerical models. European Journal of Civil engineering 18 (10) (2014) 1177 - 1191
[22] de Larrard, T., J. B. Colliat, F. Benboudjema, J. M. Torrenti, et G. Nahas Effect of the young modulus variability on the mechanical behaviour of a nuclear containment vessel. Nuclear engineering and Design 240(12) (2010) 4051–4060
[23] Ghanem, R., Spanos, P. Stochastic finite elements – A spectral approach. Revised edition. Dover Publications, INC. New York. USA, 1991.
[24] Baroth J., Breysse D., Schoefs F. Construction Reliability: Safety, Variability and Sustainability. 2011. Wiley-ISTE. ISBN: 978-1-84821-230-5.